

Acoustics'08
Paris
June 29-July 4, 2008

www.acoustics08-paris.org

euronoise

Active Sound Field Equalization

Akira Omoto, Hisaharu Suzuki and Akihiro Kakiuchi

Kyushu University, 4-9-1, Shiobaru, Minamiku, 815-8540 Fukuoka, Japan
omoto@design.kyushu-u.ac.jp

The concept and the preliminary examination of active sound field equalization are presented. As well known, active control scheme is mostly used for suppressing the sound pressure at certain points. In our method, however, the sound pressure and the particle velocity are adopted as the control quantity. The acoustic intensities or the specific acoustic impedances at plural points are then modified to control the directional characteristics of the sound field in the enclosure. As a result, the intensity controller changes the direction of standing waves. On the other hands, the impedance controller shows the tendency to yield the propagating waves in desired direction. Both methods show potentials to equalize irregularities of the sound field due to the strong acoustic modes.

1 Introduction

Active sound equalizer is often designed to compensate the irregular frequency characteristics due to the strong acoustic modes in enclosures, for example. Typical method is to make the equalization filter tracking the delayed version of the original signal[1] or the impulse response of the plane wave field[2].

Meanwhile, our system presented in this report intends to change the directional characteristics of the sound field by modifying the balance of the acoustic intensities or the specific acoustic impedances in three orthogonal directions. This concept is firstly utilized for an ‘active reverberation chamber’ in which the any desired incident angles can be achieved by active sound radiation[3]. As a ‘good side effects’ of controlling these balances, the controller is expected to perform as a effective space equalizer, since it can remove the large variations of the sound pressure in the enclosure. The formulation and the results of the numerical simulations are shown below.

2 Principle of Controller Design

2.1 Expression of Controlled Field

Assume the multi-channel active control system which consists of L error sensors and M secondary sources as shown in Fig. 1. The number of primary source is assumed as one. The sound pressure and the particle velocity in x direction at ℓ -th error sensor, $p_\ell, v_{x,\ell}$ can be expressed in the frequency domain expression as

$$p_\ell = d_{p,\ell} + \sum_{m=1}^M g_{p,\ell,m} \cdot q_m \quad (1)$$

$$v_{x,\ell} = d_{x,\ell} + \sum_{m=1}^M g_{x,\ell,m} \cdot q_m, \quad (2)$$

where, $d_{p,\ell}$ and $d_{x,\ell}$ are the primary sound pressure and particle velocity in x direction. The $g_{p,\ell,m}$ is the transfer function from m -th secondary source to ℓ -th error sensor. This transfer function converts m -th source strength q_m to sound pressure. Similarly, the $g_{x,\ell,m}$ is the transfer function from m -th secondary source to ℓ -th error sensor for particle velocity in x -direction. The sound pressures and the particle velocities in $x, y,$ and z direction at L sensors can be arranged in vector-matrix form as

$$\mathbf{p} = \mathbf{d}_p + \mathbf{G}_p \mathbf{q}, \quad (3)$$

$$\mathbf{v}_x = \mathbf{d}_x + \mathbf{G}_x \mathbf{q}, \quad (4a)$$

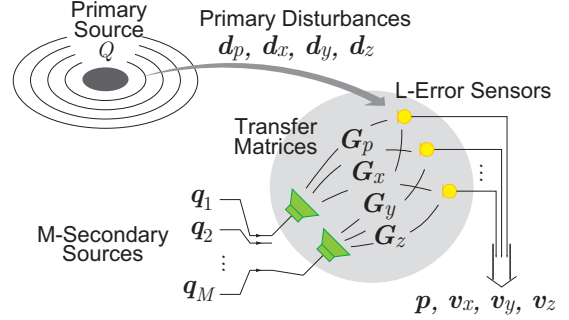


Figure 1: Block diagram of the control system in which the L -error sensors, M -secondary sources are assumed.

$$\mathbf{v}_y = \mathbf{d}_y + \mathbf{G}_y \mathbf{q}, \quad (4b)$$

$$\mathbf{v}_z = \mathbf{d}_z + \mathbf{G}_z \mathbf{q}, \quad (4c)$$

where $\mathbf{p} = [p_1 \ p_2 \ \dots \ p_L]^T$, $\mathbf{v}_x = [v_{x,1} \ v_{x,2} \ \dots \ v_{x,L}]^T$, $\mathbf{d}_p = [d_{p,1} \ d_{p,2} \ \dots \ d_{p,L}]^T$, $\mathbf{d}_x = [d_{x,1} \ d_{x,2} \ \dots \ d_{x,L}]^T$,

$$\mathbf{G}_p = \begin{bmatrix} g_{p,1,1} & g_{p,1,2} & \dots & g_{p,1,M} \\ g_{p,2,1} & g_{p,2,2} & \dots & g_{p,2,M} \\ \vdots & \vdots & \ddots & \vdots \\ g_{p,L,1} & g_{p,L,2} & \dots & g_{p,L,M} \end{bmatrix}, \quad (5)$$

$$\mathbf{G}_x = \begin{bmatrix} g_{x,1,1} & g_{x,1,2} & \dots & g_{x,1,M} \\ g_{x,2,1} & g_{x,2,2} & \dots & g_{x,2,M} \\ \vdots & \vdots & \ddots & \vdots \\ g_{x,L,1} & g_{x,L,2} & \dots & g_{x,L,M} \end{bmatrix} \quad (6)$$

and $\mathbf{q} = [q_1 \ q_2 \ \dots \ q_M]^T$. The velocities and transfer functions for y and z directions are defined similarly.

Free field If we assume the point primary source at the location of (x_0, y_0, z_0) in the free field, the primary field at the ℓ -th error sensor $(x_{e,\ell}, y_{e,\ell}, z_{e,\ell})$ can be expressed as

$$d_{p,\ell} = \frac{j\omega\rho_0 Q}{4\pi} \frac{e^{-jkr_{0,\ell}}}{r_{0,\ell}}, \quad (7)$$

$$d_{x,\ell} = \frac{Q}{4\pi} \frac{1 + jkr_{0,\ell} \frac{x_{e,\ell} - x_0}{r_{0,\ell}}}{r_{0,\ell}^2} e^{-jkr_{0,\ell}}, \quad (8a)$$

$$d_{y,\ell} = \frac{Q}{4\pi} \frac{1 + jkr_{0,\ell} \frac{y_{e,\ell} - y_0}{r_{0,\ell}}}{r_{0,\ell}^2} e^{-jkr_{0,\ell}}, \quad (8b)$$

$$d_{z,\ell} = \frac{Q}{4\pi} \frac{1 + jkr_{0,\ell} \frac{z_{e,\ell} - z_0}{r_{0,\ell}}}{r_{0,\ell}^2} e^{-jkr_{0,\ell}}, \quad (8c)$$

where $j = \sqrt{-1}$, ω is an angular frequency, ρ_0 is a mass density of the medium (air), Q is the primary source strength, k is a wavenumber, and

$$r_{0,\ell} = \sqrt{(x_{e,\ell} - x_0)^2 + (y_{e,\ell} - y_0)^2 + (z_{e,\ell} - z_0)^2}.$$

The elements of transfer functions are expressed as

$$g_{p,\ell,m} = \frac{j\omega\rho_0 e^{-jkr_{sm,\ell}}}{4\pi r_{sm,\ell}} \quad (9)$$

$$g_{x,\ell,m} = \frac{1}{4\pi} \frac{1 + jkr_{sm,\ell}}{r_{sm,\ell}^2} \frac{x_{e,\ell} - x_{sm}}{r_{sm,\ell}} e^{-jkr_{sm,\ell}}, \quad (10a)$$

$$g_{y,\ell,m} = \frac{1}{4\pi} \frac{1 + jkr_{sm,\ell}}{r_{sm,\ell}^2} \frac{y_{e,\ell} - y_{sm}}{r_{sm,\ell}} e^{-jkr_{sm,\ell}}, \quad (10b)$$

$$g_{z,\ell,m} = \frac{1}{4\pi} \frac{1 + jkr_{sm,\ell}}{r_{sm,\ell}^2} \frac{z_{e,\ell} - z_{sm}}{r_{sm,\ell}} e^{-jkr_{sm,\ell}}, \quad (10c)$$

provided the m -th secondary source is located at (x_{sm}, y_{sm}, z_{sm}) and

$$r_{sm,\ell} = \sqrt{(x_{e,\ell} - x_{sm})^2 + (y_{e,\ell} - y_{sm})^2 + (z_{e,\ell} - z_{sm})^2}.$$

Lightly damped enclosure Another important example used in this report is a lightly damped rectangular enclosure whose transfer functions can be evaluated by the modal summation method [4]. Assume the dimensions of the enclosure as $L_x \times L_y \times L_z$. The modal function of the enclosure at the receiving position (x, y, z) , can be calculated as

$$\psi_{p,n}(x, y, z) = \epsilon_n \cos \frac{n_x \pi x}{L_x} \cos \frac{n_y \pi y}{L_y} \cos \frac{n_z \pi z}{L_z}, \quad (11)$$

$$\psi_{x,n}(x, y, z) = \frac{1}{j\omega\rho_0} \frac{n_x \pi}{L_x} \epsilon_n \sin \frac{n_x \pi x}{L_x} \cos \frac{n_y \pi y}{L_y} \cos \frac{n_z \pi z}{L_z}, \quad (12a)$$

$$\psi_{y,n}(x, y, z) = \frac{1}{j\omega\rho_0} \frac{n_y \pi}{L_y} \epsilon_n \cos \frac{n_x \pi x}{L_x} \sin \frac{n_y \pi y}{L_y} \cos \frac{n_z \pi z}{L_z}, \quad (12b)$$

$$\psi_{z,n}(x, y, z) = \frac{1}{j\omega\rho_0} \frac{n_z \pi}{L_z} \epsilon_n \cos \frac{n_x \pi x}{L_x} \cos \frac{n_y \pi y}{L_y} \sin \frac{n_z \pi z}{L_z}, \quad (12c)$$

where n_x, n_y, n_z are the independently increasing integers from zero, and the normalizing factor $\epsilon_n = \sqrt{\epsilon_x \cdot \epsilon_y \cdot \epsilon_z}$ and $\epsilon_{(x,y,z)} = 1$ and $\epsilon_{(x,y,z)} = 2$ for the cases of $n_{(x,y,z)} = 0$ and $n_{(x,y,z)} > 0$ respectively. Then the primary field can be expressed as

$$d_{p,\ell} = Q \sum_{n=0}^N a_n \psi_{p,n}(x_{e,\ell}, y_{e,\ell}, z_{e,\ell}) \quad (13)$$

$$d_{x,\ell} = Q \sum_{n=0}^N a_n \psi_{x,n}(x_{e,\ell}, y_{e,\ell}, z_{e,\ell}), \quad (14a)$$

$$d_{y,\ell} = Q \sum_{n=0}^N a_n \psi_{y,n}(x_{e,\ell}, y_{e,\ell}, z_{e,\ell}), \quad (14b)$$

$$d_{z,\ell} = Q \sum_{n=0}^N a_n \psi_{z,n}(x_{e,\ell}, y_{e,\ell}, z_{e,\ell}). \quad (14c)$$

In the summation above, the integer $n = 0$ if $n_x = n_y = n_z = 0$ and increases with any different combination of n_x, n_y and n_z . The coefficient a_n associated with the location of the source can be expressed as

$$a_n = \frac{\omega\rho_0 c^2 \psi_{p,n}(x_0, y_0, z_0)}{L_x L_y L_z [2\zeta_n \omega_n \omega + j(\omega^2 - \omega_n^2)]}, \quad (15)$$

where c is the sound speed, ζ_n is the damping ratio of n -th mode, and ω_n is the natural angular frequency which can be calculated as

$$\omega_n = c \sqrt{\left(\frac{n_x \pi}{L_x}\right)^2 + \left(\frac{n_y \pi}{L_y}\right)^2 + \left(\frac{n_z \pi}{L_z}\right)^2} \quad (16)$$

The elements of transfer matrices are expressed as

$$g_{p,\ell,m} = \sum_{n=0}^N B_{m,n} \psi_{p,n}(x_{e,\ell}, y_{e,\ell}, z_{e,\ell}), \quad (17)$$

$$g_{x,\ell,m} = \sum_{n=0}^N B_{m,n} \psi_{x,n}(x_{e,\ell}, y_{e,\ell}, z_{e,\ell}), \quad (18a)$$

$$g_{y,\ell,m} = \sum_{n=0}^N B_{m,n} \psi_{y,n}(x_{e,\ell}, y_{e,\ell}, z_{e,\ell}), \quad (18b)$$

$$g_{z,\ell,m} = \sum_{n=0}^N B_{m,n} \psi_{z,n}(x_{e,\ell}, y_{e,\ell}, z_{e,\ell}), \quad (18c)$$

where

$$B_{m,n} = \frac{\omega\rho_0 c^2 \psi_{p,n}(x_{sm}, y_{sm}, z_{sm})}{L_x L_y L_z [2\zeta_n \omega_n \omega + j(\omega^2 - \omega_n^2)]}. \quad (19)$$

2.2 Control Strategy

The normal Active Noise Control (ANC) scheme intend to reduce the sum of the squared pressure $\mathbf{p}^H \mathbf{p}$ and the optimum secondary source strength are known as [4]

$$\mathbf{q}_{\min,p} = -[\mathbf{G}_p^H \mathbf{G}_p]^{-1} \mathbf{G}_p^H \mathbf{d}_p \quad (20)$$

Intensity Control We assume here the cost function J as the multiplication of the sound pressure vector and weighted particle velocities as

$$J = [\mathbf{p}^H \mathbf{p}^H \mathbf{p}^H] \begin{bmatrix} w_x \mathbf{v}_x \\ w_y \mathbf{v}_y \\ w_z \mathbf{v}_z \end{bmatrix} = [\mathbf{d}_p + \mathbf{G}_p \mathbf{q}]^H [\mathbf{d}_v + \mathbf{G}_v \mathbf{q}], \quad (21)$$

where w_x, w_y, w_z are the weighting value of the intensities for each direction, and

$$\mathbf{d}_v = w_x \mathbf{d}_x + w_y \mathbf{d}_y + w_z \mathbf{d}_z, \quad (22)$$

$$\mathbf{G}_v = w_x \mathbf{G}_x + w_y \mathbf{G}_y + w_z \mathbf{G}_z. \quad (23)$$

This cost function can be expressed 'quasi' quadratic form as

$$J = \mathbf{q}^H \mathbf{A} \mathbf{q} + \mathbf{q}^H \mathbf{B} + \mathbf{C} \mathbf{q} + \mathbf{D} \quad (24)$$

where $\mathbf{A} = \mathbf{G}_p^H \mathbf{G}_p$, $\mathbf{B} = \mathbf{G}_p^H \mathbf{d}_v$, $\mathbf{C} = \mathbf{d}_p^H \mathbf{G}_v$ and $\mathbf{D} = \mathbf{d}_p^H \mathbf{d}_v$. Note that there is no guarantee that the matrix \mathbf{A} is positive definite nor having its inverse. The individual examinations are needed to verify the proposed method.

Anyway, the 'optimum' strength vector $\mathbf{q}_{\min,intensity}$ can be calculated as

$$\mathbf{q}_{\min,intensity} = -[\mathbf{G}_p^H \mathbf{G}_p]^{-1} \mathbf{G}_p^H \mathbf{d}_v \quad (25)$$

Assume that the weighting are set as $w_x = 1, w_y = 0, w_z = 0$, then the calculated controller Eq. (25) reduces only the intensity in x direction. Any combination of weightings has possibilities to change the direction of energy flow of sound.

Impedance control We define the error function as the difference between sound pressure and the weighted particle velocities multiplied by the characteristic impedance of the medium, Z_0 as

$$\mathbf{e} = \mathbf{p} - Z_0 (w_x \mathbf{v}_x + w_y \mathbf{v}_y + w_z \mathbf{v}_z). \quad (26)$$

If we set the weights as $w_x = 1, w_y = 0, w_z = 0$, the controller tend to modify the relation of sound pressure and the particle velocity as $\mathbf{p} - Z_0 \mathbf{v}_x = 0$ and therefore, $\mathbf{p}/\mathbf{v}_x = Z_0$, i.e., the feature of plane propagating wave in x direction.

The error function can be manipulated into

$$\mathbf{e} = \mathbf{d}_{imp} + \mathbf{G}_{imp} \mathbf{q}, \quad (27)$$

where $\mathbf{d}_{imp} = \mathbf{d}_p - Z_0 (w_x \mathbf{d}_x + w_y \mathbf{d}_y + w_z \mathbf{d}_z)$, and $\mathbf{G}_{imp} = \mathbf{G}_p - Z_0 (w_x \mathbf{G}_x + w_y \mathbf{G}_y + w_z \mathbf{G}_z)$. The optimum secondary source strength to minimize the squared sum of the error function $\mathbf{e}^H \mathbf{e}$ can be derived as

$$\mathbf{q}_{\min, impedance} = - [\mathbf{G}_{imp}^H \mathbf{G}_{imp}]^{-1} \mathbf{G}_{imp}^H \mathbf{d}_{imp} \quad (28)$$

3 Numerical Simulation

To verify the validity of the proposed method, the numerical simulations were performed in the simple two-dimensional sound field. We assumed the extremely ‘modal’ condition, in which the dimensions of the enclosure were $L_x = L_y = 1$ [m], $L_z = 0.05$ [m] and the excitation frequency was set to 240 Hz (the wavelength $\lambda = 1.42$ m).

Simple arrangement of the sources The primary source was located at one corner and the three secondary sources were located remaining corners as shown in Fig. 2 (a). These sources were designed to control the intensity and the impedance at the four points sensors. Transfer functions are calculated by Eqs. (11) to (19) and n_z was set to zero. The weighting parameter w_x, w_y were determined as $(w_x, w_y) = (\cos \theta, \sin \theta)$ and the angle θ was set to $0^\circ, 35^\circ, 45^\circ, 55^\circ$ and 90° , as examples.

Figure 3 shows the results. The top left figure shows the primary distribution of sound pressure levels and the directions of sound intensities by the arrows. The left and the right columns corresponds to the impedance and the intensity control, respectively. The each row indicates the results of each angle, θ . As mentioned in the previous section, the weighting parameters of $(w_x, w_y) = (\cos \theta, \sin \theta)$ would result that; the impedance controller tends to make the ratio of the sound pressure and the particle velocity to Z_0 , in set direction, and the intensity controller tends to reduce the set angle intensity.

The results of the intensity control show that the reduction of the intensity in certain direction made the remaining intensity being prominent. On the other hand, the impedance controller make the sound field being relatively smooth and flat field. Additionally, the intensity arrows tend to point the desired direction in the wide area inside the enclosure.

The sum of the squared source strengths, $\mathbf{q}^H \mathbf{q}$ were drawn for various set of angles and the excitation frequencies in Fig. 4. The -20 dB in the vertical axis

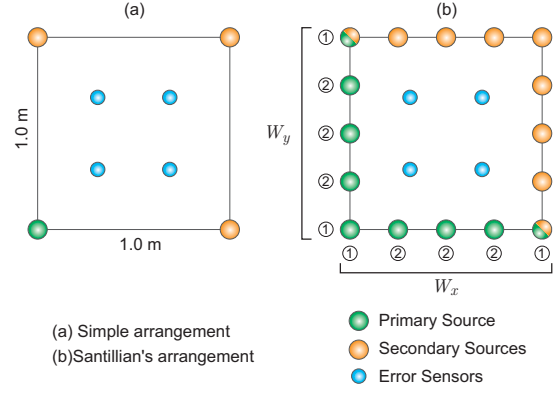


Figure 2: Arrangement of the primary source, the secondary sources, and the error sensors.

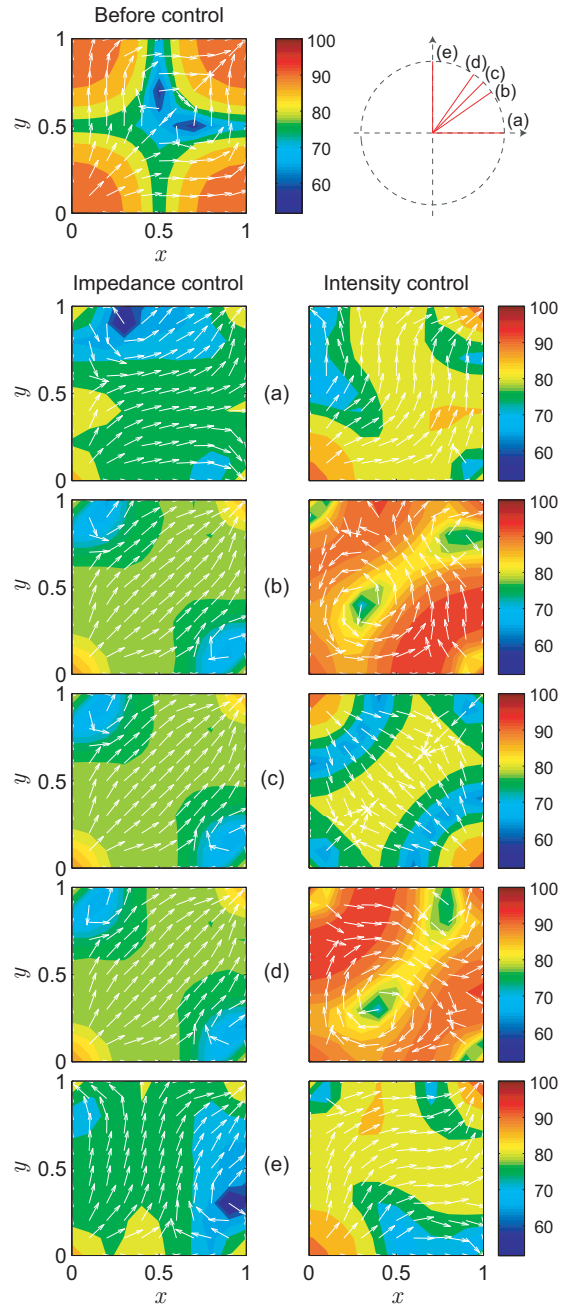


Figure 3: Results of the numerical simulation with simple source arrangement.

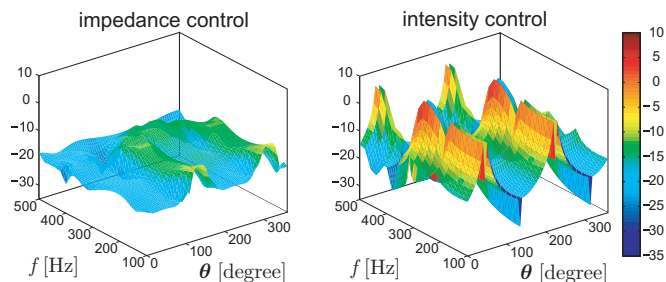


Figure 4: Sum of the squared source strength for the intensity and the impedance control.

corresponds to the level of the primary source strength. Apparently, intensity control had steep peaks and dips depending on the set angle and the frequency. The impedance control looks being more well-balanced control strategy.

Santillán's arrangement A distinctive sound field control method was proposed by Santillán[5, 6]. His method used widely distributed loudspeakers having strength which corresponded to their assigned solid angle. In this section, we try to combine his idea and our control method.

Firstly, we assume that two orthogonal walls are covered with source arrays which have weightings as introduced by Santillán as shown in Fig. 2 (b). The numbers in the circles indicate the fundamental weighting. To realize the arbitrary directional feature in the primary field, the multiplicative weighting W_x and W_y are assumed, i.e., if we intend to generate the primary field of direction θ , then the W_x and W_y are calculated as

$$W_x = \frac{\cos \theta}{|\cos \theta| + |\sin \theta|}, \quad W_y = \frac{\sin \theta}{|\cos \theta| + |\sin \theta|}. \quad (29)$$

The secondary sources are arranged symmetrical location with primary sources. The number of secondary sources are nine and they are driven with the strength to control the intensity and the impedance at four points in the enclosure. Results are shown in Fig. 5. Only the results of the impedance control are shown. The left column shows the distribution of sound pressure and the intensity before control. The angle θ is set to (a) 0° , (b) 30° , (c) 45° , (d) 60° , (e) 90° , (f) 120° , (g) 135° , (h) 150° , and (i) 180° .

Apparently, the weighting for primary source W_x and W_y generated the sound field of desired directivity features. However, the modes in each direction resulted in the variation of sound pressure levels more than 20 dB. Also, the sound pressure in the case of (g) 135° fell greatly.

Impedance controller, however, showed the effective 'equalization' of sound field with energy flow of desired directions. The extremely reduced sound pressure at the primary field of (g) 135° was compensated by the impedance controller.

4 Concluding Remarks

Active control of acoustic intensity and impedance were proposed. Both method could change the directivity

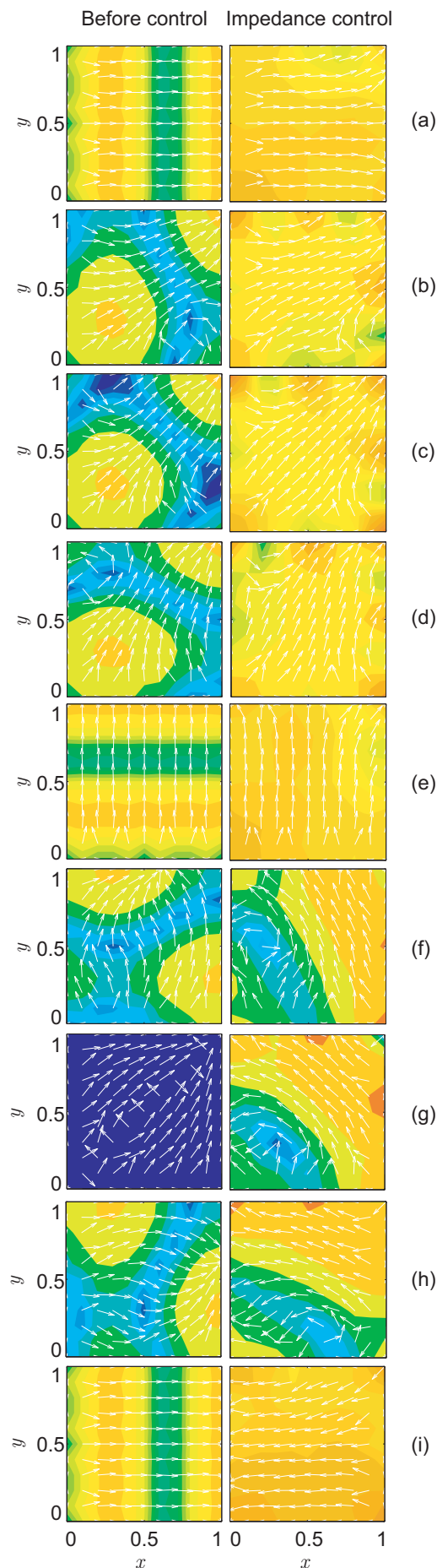


Figure 5: Results of the numerical simulation with Santillán's arrangement.

features of the sound field in the enclosure. Especially, the impedance controller showed possibilities of realizing effective sound field equalizer which can equalize the sound pressure distribution even for the low modal density case. These results suggested that the impedance controller yielded the equivalent propagative sound field in arbitrary angle.

The adaptive implementation of control strategy and physical interpretation of the obtained results are the current subject of our research.

References

- [1] S. J. Elliott, P. A. Nelson, "Multiple-point equalization in a room using adaptive digital filters," *J. Audio Eng. Soc.* 37 (11), 899–907 (1989).
- [2] O. Kirkeby, P. A. Nelson, "Reproduction of plane wave sound field," *J. Acoust. Soc. Am.*, 94 (5), 2992–3000 (1993).
- [3] H. Suzuki, A. Omoto, and K. Fujiwara, "Concept of active reverberation box," *J. Acoust. Soc. Am.*, 120 (5), Pt.2, 3188 (2006).
- [4] P. A. Nelson, S. J. Elliott, *Active Control of Sound*, Academic Press, 1992.
- [5] A. O. Santillán, "Spatially extended sound equalization in rectangular rooms," *J. Acoust. Soc. Am.* 110 (4), 1989–1997 (2001).
- [6] A. O. Santillán, et al., "Experimental implementation of a low-frequency global sound equalization method based on free field propagation," *Applied Acoustics*, 68, 1063–1085 (2007).